Supplementary Material

Nonvolatile electrical control of electronic and valleytronic properties by ferroelectricity in the VSi_2P_4/Al_2S_3 van der Waals heterostructure

Shoubao Zhang[a], Na Jiao[a], Hongyan Lu[a], Mengmeng Zheng[a], Ping Zhang[ab], Meiyan Ni[a*]
[a] School of Physics and Physical Engineering, Qufu Normal University, Qufu 273165, China
[b]Institute of Applied Physics and Computational Mathematics, Beijing 100088, China
Email: nimy@qfnu.edu.cn (MY. Ni)

1. Phonon spectra, magnetic configurations, and energy difference of different magnetic configurations of VSi_2P_4 and Al_2S_3 monolayer

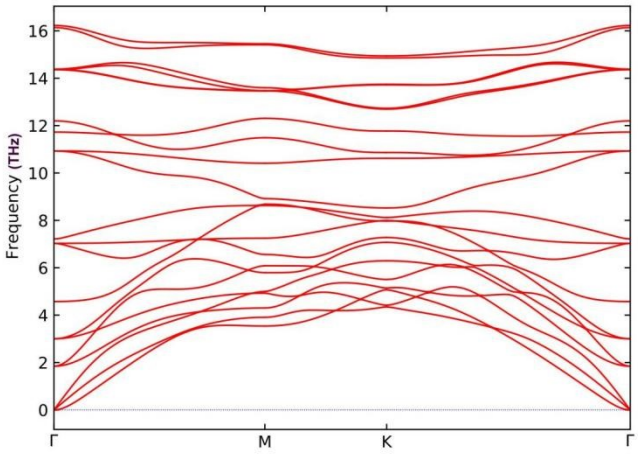

Fig. S1 Phonon spectrum of VSi_2P_4 monolayer.

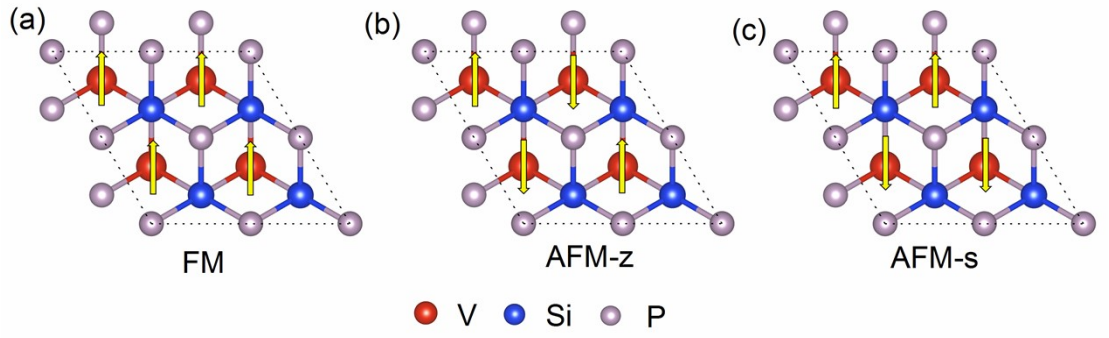

Fig. S2 Different magnetic configurations of monolayer VSi_2P_4 for (a) ferromagnetic, (b) zigzag-antiferromagnetic, (c) stripe-antiferromagnetic congfigurations. The yellow arrow represents the direction of the magnetic moment.

Table S1 The energy difference $\Delta E = E - E_{FM}$ (in units of eV) of VSi_2P_4 monolayer with different magnetic states.

	FM	NM	AFM-z	AFM-s
ΔE	0	0.106	0.013	0.013

Table. S2: Distribution of magnetic moment on each atom of VSi_2P_4 monolayer, UP-1 HS and DW-1 HS.(the unit: μ_B)

	Total	V atom	Si atom	P atom	
Monolayer VSi_2P_4	0.933	1.106	0.006 0.006	-0.090 -0.002	-0.090 -0.002
UP-1	0.926	1.092	0.006 0.006	-0.087 -0.002	-0.087 -0.002
DW-1	0.939	1.110	0.006 0.006	-0.088 -0.002	-0.088 -0.002

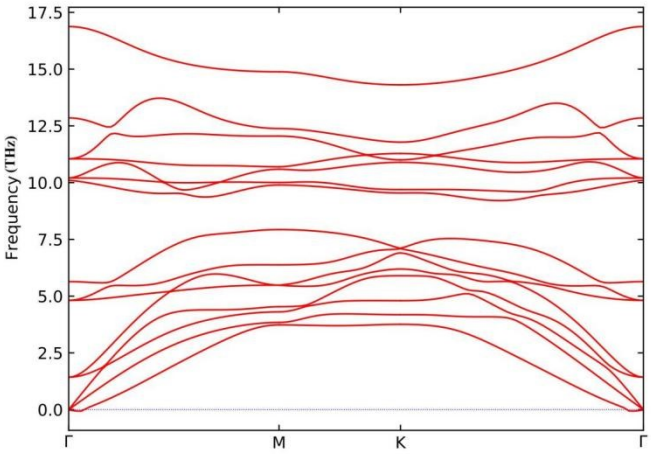

Fig. S3 phonon spectrum of Al_2S_3 monolayer.

2. Band structures of VSi_2P_4 and Al_2S_3 monolayers calculated by HSE06 method

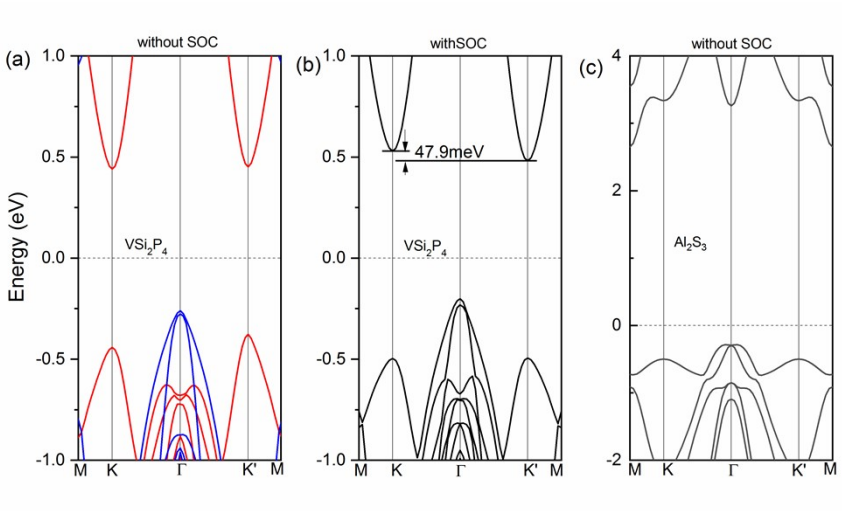

Fig. S4 Band structures calculated by the hybrid functional (HSE06) method: panel (a) and (b) are for the VSi_2P_4 monolayer without and with SOC, and panel (c) is for the Al_2S_3 monolayer without SOC.

3. Various configurations of the VSi_2P_4 /Al_2S_3 heterostructure and the energy difference of VSi_2P_4 /Al_2S_3 heterostructures with different magnetic states

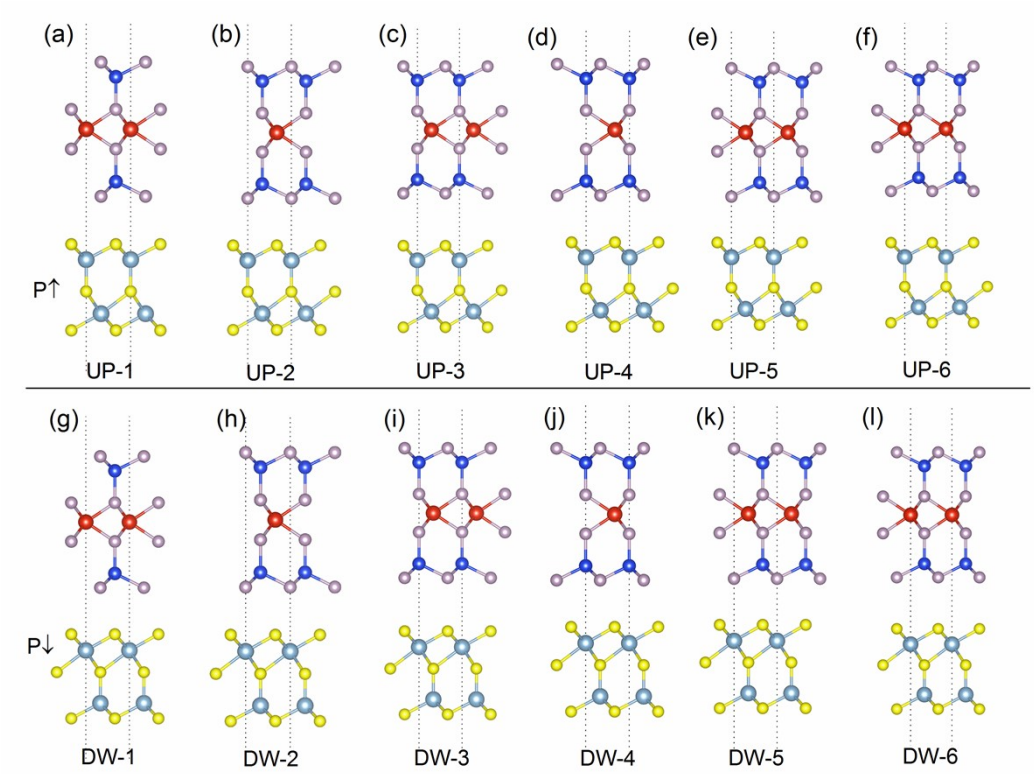

Fig. S5 Six stacking configurations of the VSi_2P_4/Al_2S_3 heterostructures (side view). (a)-(f) show six stacking configurations with the electric polarization of Al_2S_3 upwards. (g)-(l) show six stacking configurations with the electric polarization of Al_2S_3 downwards.

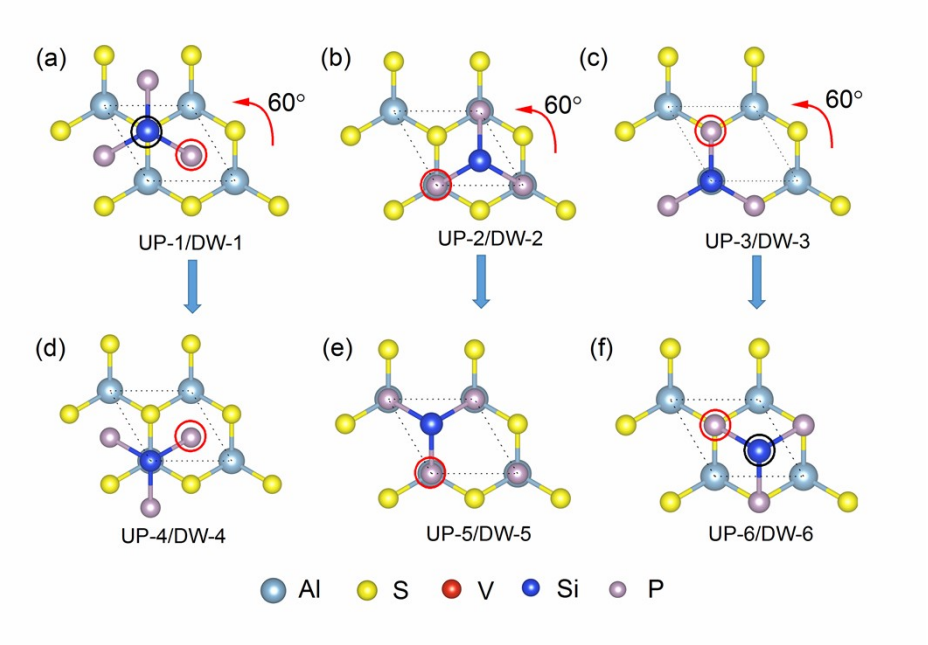

Fig. S6 Six stacking configurations of the VSi_2P_4/Al_2S_3 heterostructures (top view). To make it clear, just two adjacent layers of VSi_2P_4 and Al_2S_3 are shown. Configurations (d-f) are obtained by rotating 60° counterclockwise of VSi_2P_4 in configurations (a-c) with P atom (in red circle) as the center with Al_2S_3 unmoved.

Table S3 The energy difference $\Delta E = E - E_{FM}$ (in units of eV) of UP-1 and DW-1 heterostructures with different magnetic states.

	FM	NM	AFM-z	AFM-s
UP-1	0	0.992	0.130	0.130
DW-1	0	0.868	0.132	0.232

Table S4 The energy difference $\Delta E = E - E_{UP-1(DW-1)}$ of heterostructures with different stacking configurations.

configuration	UP-1	UP-2	UP-3	UP-4	UP-5	UP-6
$\Delta E(meV)$	0	2.3	56.0	4.4	0.7	56.5
configuration	DW-1	DW-2	DW-3	DW-4	DW-5	DW-6
$\Delta E(meV)$	0	6.5	58.7	2.1	2.8	59.1

4. Band structures and charge density differenceof the VSi_2P_4/Al_2S_3 heterostructures

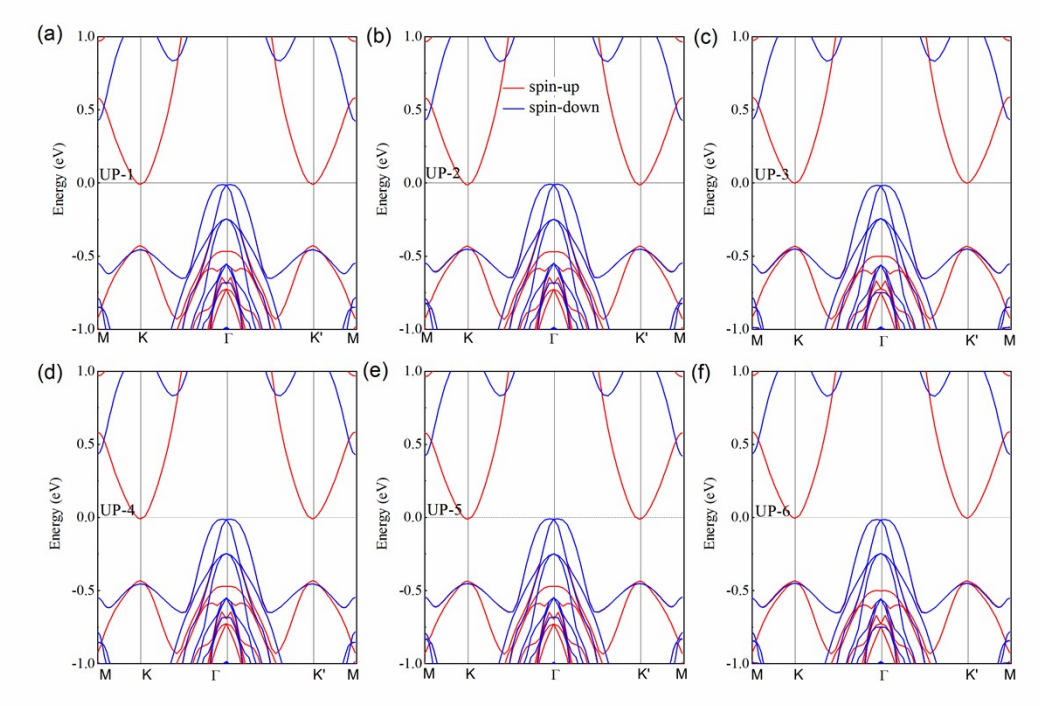

Fig. S7. Electronic band structures of the configurations UP-1 to UP-6 without considering SOC. Red and blue lines represent the spin-up and spin-down channels of HSs.

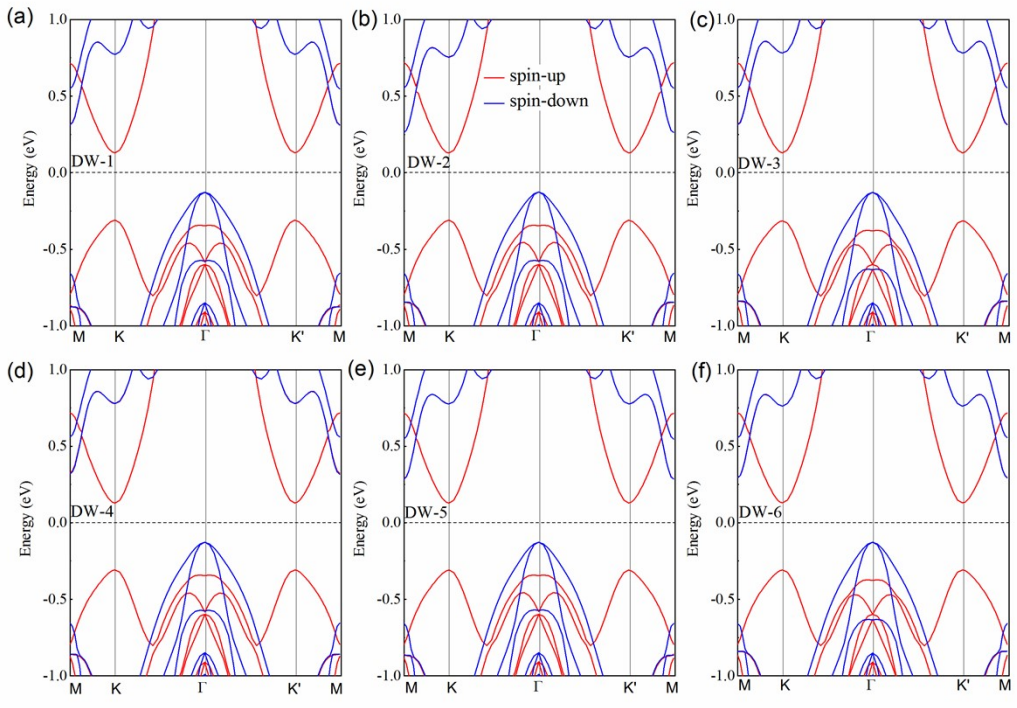

Fig. S8. Electronic band structures of the configurations DW-1 to DW-6 without considering SOC. Red and blue lines represent the spin-up and spin-down channels of HSs.

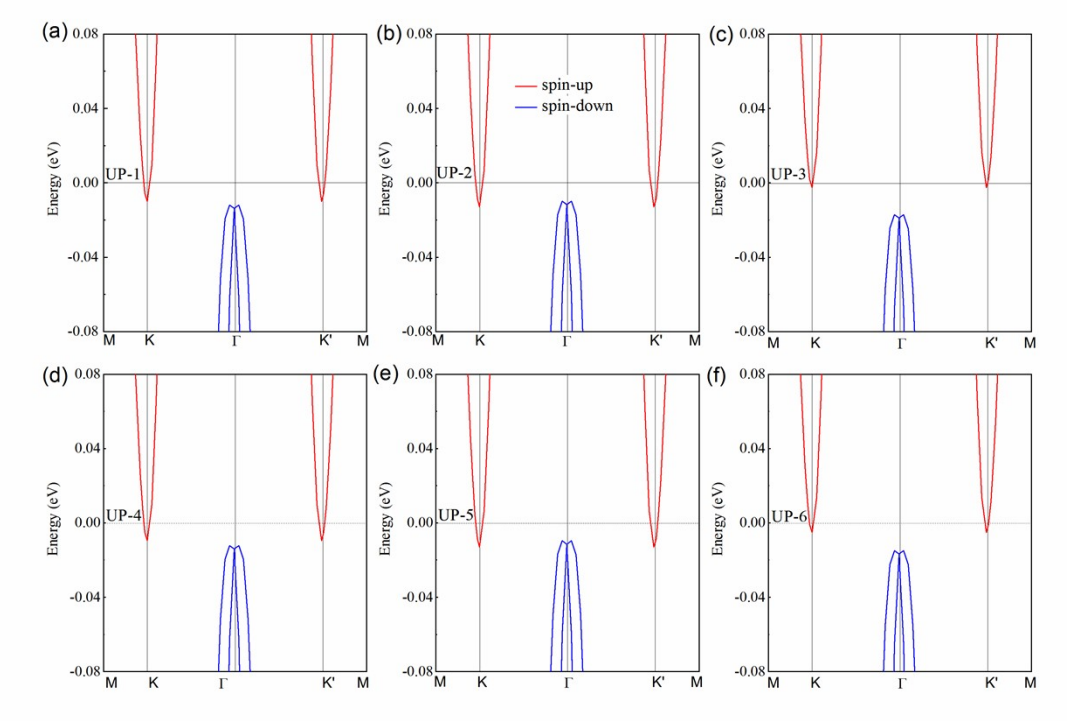

Fig. S9. Electronic band structures of the configurations UP-1 to UP-6 without considering SOC. Compared with Fig. S5, the range of the energy of this figure is limited around the Fermi level. Red and blue lines represent the spin-up and spin-down channels of HSs.

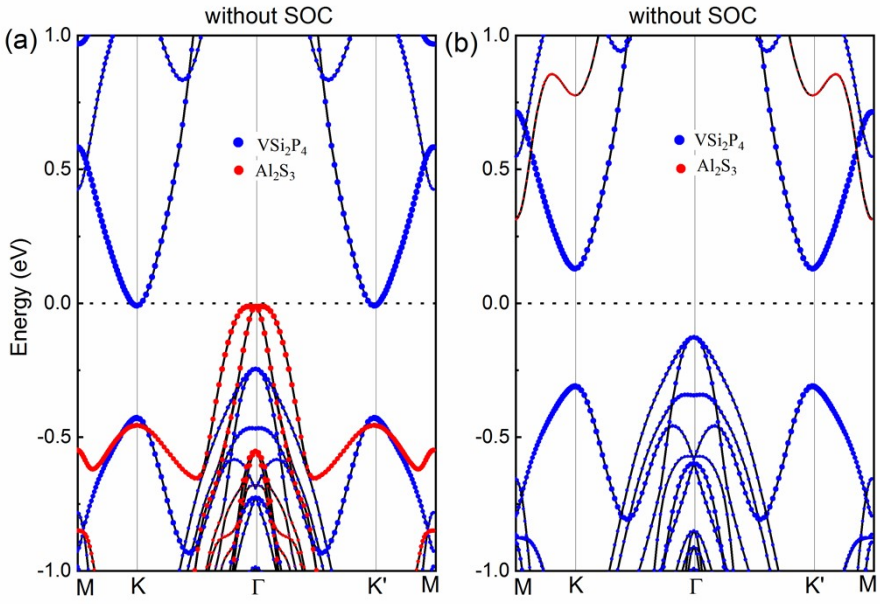

Fig. S10 Projected band structures of (a) UP-1 and (b) DW-1 configurations without SOC. Red and blue lines represent the contributions from spin-up and spin-down channel, and the blue and red dots denote the contributions from VSi_2P_4 and Al_2S_3.

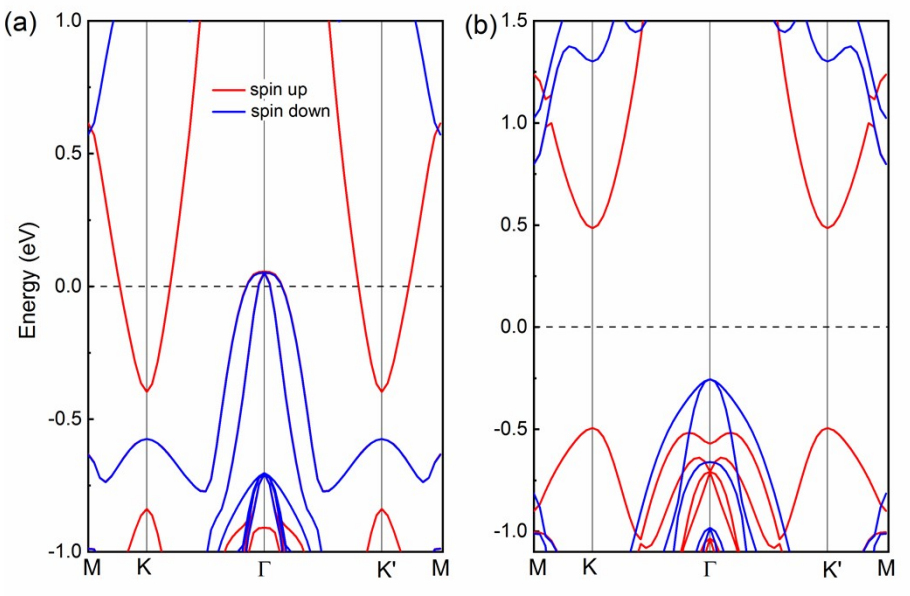

Fig. S11. Electronic band structures of the configurations UP-1 to UP-6 with HSE06 method. Red and blue lines represent the spin-up and spin-down channels of HSs.

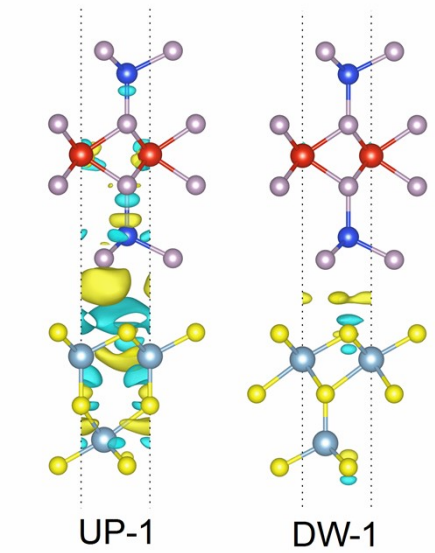

Fig. S12 The charge density difference of UP-1 annd DW-1 heterostructures. The blue and yellow distributions represent the charge depletion and accumulation with an isosurface value of 1.2×10^{-4} e $Å^{-3}$, respectively.

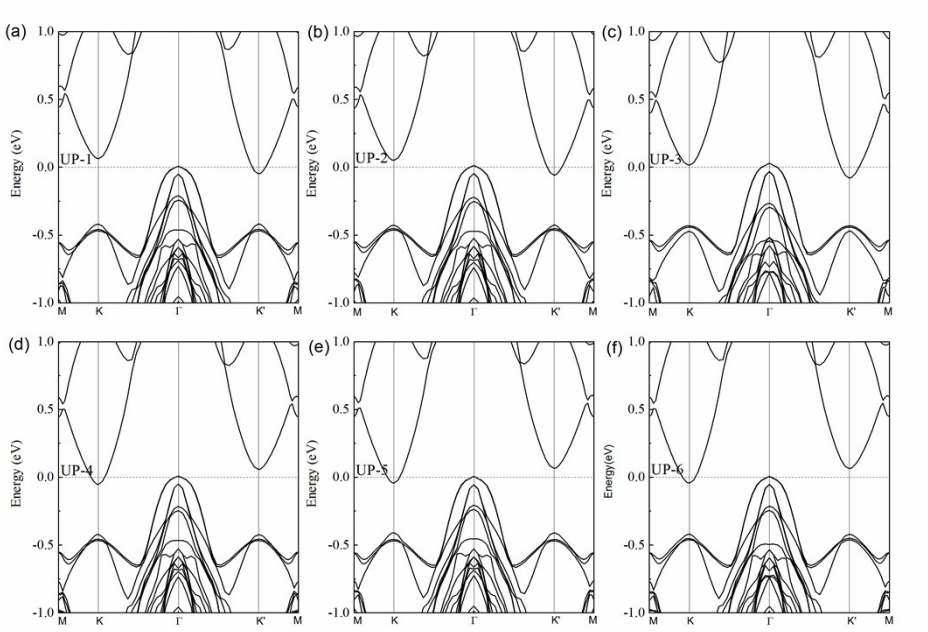

Fig. S13. Electronic band structures of the configurations UP-1 to UP-6 considering SOC.

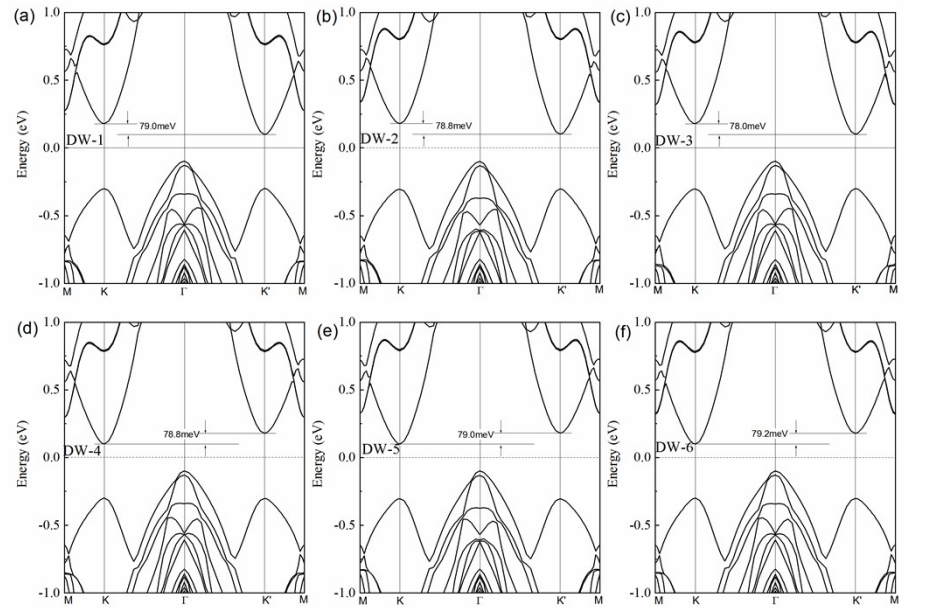

Fig. S14. Electronic band structures of the configurations DW-1 to DW-6 considering SOC.